nrp Nutrition Research and Practice

Original Research

Check for updates

Protaetia brevitarsis larvae extract protects against lipopolysaccharides-induced ferroptosis and inflammation by inhibiting acid sphingomyelinase

Woo-Jae Park [iD] [1§], **Eunyoung Oh** [iD] [2,3], and **Yookyung Kim** [iD] [3§]

[1]Department of Biochemistry, Chung-Ang University College of Medicine, Seoul 06974, Korea
[2]Interdisciplinary Program in Sustainable Living System, Graduate School, Korea University, Seoul 02841, Korea
[3]Department of Human Ecology, Graduate School, Korea University, Seoul 02841, Korea

OPEN ACCESS

§**Corresponding Authors:**

Woo-Jae Park
Department of Biochemistry, Chung-Ang University College of Medicine, 84 Heukseok-ro, Dongjak-gu, Seoul 06974, Korea.
Tel. +82-2-820-5308
Email. ooze@cau.ac.kr

Yookyung Kim
Department of Human Ecology, Graduate School, Korea University, 145 Anam-ro, Seongbuk-gu, Seoul 02841, Korea.
Tel. +82-2-3290-2328
Email. yookyung_kim@korea.ac.kr

ORCID iDs
Woo-Jae Park [iD]
https://orcid.org/0000-0002-5770-7096
Eunyoung Oh [iD]
https://orcid.org/0009-0004-1357-991X
Yookyung Kim [iD]
https://orcid.org/0000-0002-8438-0121

ABSTRACT

BACKGROUND/OBJECTIVES: Inflammation and ferroptosis are implicated in various diseases and lipopolysaccharides (LPS) have been linked with these disorders. Recently, many edible insects, such as *Gryllus bimaculatus, Protaetia brevitarsis* larvae (PB) and *Tenebrio molitor* larvae, have been recommended as alternative foods because they contain lots of nutritional sources. In this study, we explored the potential of PB extract in preventing LPS-induced inflammation and ferroptosis in Hep3B cells.
MATERIALS/METHODS: PB powder was extracted using 70% ethanol and applied to Hep3B cells. Co-treatment with LPS was conducted to induce ferroptosis and inflammation. The anti-inflammatory and anti-ferroptosis mechanisms of the PB extract were confirmed using Western blot, enzyme-linked immunosorbent assay, and real-time polymerase chain reaction analysis.
RESULTS: PB extract effectively prevented LPS-induced cell death and restored LPS-induced inflammatory cytokine production, NF-κB signaling, endoplasmic reticulum (ER) stress and ferroptosis. Interestingly, PB extract reduced LPS-induced ceramide increase and acid sphingomyelinase (ASMase) expression. The use of the ASMase inhibitor, desipramine, also demonstrated a reduction in these pathways, highlighting the pivotal role of ASMase in inflammation and ferroptosis. Treatment with each inhibitor revealed that ferroptosis causes ER stress and that NF-κB and MAP kinase pathways are involved in inflammation.
CONCLUSION: PB emerges as a potential functional food with inhibitory effects on LPS-induced inflammation and ferroptosis, making it a promising candidate for nutritional interventions.

Keywords: Edible Insects; ceramide; sphingomyelin phosphodiesterase; ferroptosis; inflammation

INTRODUCTION

Edible insects are now emerging as alternative food sources due to their nutritional content, including proteins, fats, and minerals [1]. Moreover, the production of edible insects results in lower emissions of carbon dioxide, methane, and ammonia compared to raising traditional livestock like beef cattle and pigs [2]. Therefore, growing edible insects is environmentally friendly. Recent research has been uncovering the potential health benefits

Generated by Xmlinkpress

of edible insects, indicating a promising future for their utilization. Among the many edible insects, *Tenebrio molitor* larvae has been widely studied and found to prevent hepatic steatosis [3], obesity [4], and inflammation [5]. Similarly, *Protaetia brevitarsis* (PB) has shown promising effects on high fat diet-induced obesity [6], oxidative stress-induced hepatotoxicity [7], and attenuation of osteoclastogenesis in mouse bone marrow-derived macrophages [8]. Therefore, PB also contains various functional compounds with potential advantages against several diseases, including obesity, liver toxicity, and osteoporosis.

Lipopolysaccharide (LPS), a major component of gram-negative bacteria, is widely used for induction of inflammation. LPS not only activate inflammation by stimulating the Toll-like receptor 4 signaling pathway but also stimulates acid sphingomyelinase (ASMase) activity, increasing ceramide level [9]. ASMase hydrolyzed sphingomyelin (SM) to generate ceramide and phosphocholine [10]. ASMase is known to play an important role in many diseases, such as inflammation, tumors, cardiovascular diseases, neurological diseases, respiratory diseases, and liver diseases [10]. Studies on ASMase knockout mice have shown attenuated tumor necrosis factor (TNF)-α-mediated hepatocellular apoptosis [11], and protection against alcohol-induced liver disease [12]. Furthermore, ASMase inhibition has shown protection from Cu^{2+}-induced hepatocyte apoptosis [13]. ASMase also plays an important role in the activation of Kupffer cells [14,15]. Therefore, ASMase plays an important role in hepatocyte death and liver injury and it could be a strong candidate for many liver diseases [16]. Recent research has suggested an association between ASMase and ferroptosis [17,18], further highlighting its significance in various pathological processes.

Ferroptosis, characterized by iron-dependent cell death, is different from other forms of cell death such as apoptosis, necroptosis, and pyroptosis [19]. Its mechanism involves lipid peroxidation of unsaturated fatty acids and reduction in the levels of glutathione peroxidase 4 (GPX4), ultimately leading to iron-dependent cell death [19,20]. The interplay of these elements disrupts cellular membrane integrity and function, leading to cell death. Erastin, a well-known inducer of ferroptosis, contributes to this process by increasing the generation of reactive oxygen species (ROS) [19]. Elevated ROS levels lead to lipid peroxidation, causing the depletion of glutathione (GSH), an antioxidant that normally supports GPX4 function. As GSH levels decrease, GPX4 is downregulated, removing a key defense mechanism against lipid peroxidation [19].

Recently, it has been discovered that many edible insects have antioxidant effects [21-23]. However, no studies have been conducted on the potential effects of edible insects, such as PB, on ferroptosis. Therefore, we produced PB extract and examined the effects of PB extract on the LPS-induced inflammation and ferroptosis.

MATERIALS AND METHODS

Materials
PB larvae were obtained from GreenBugs Co-op. (Sokcho, Korea). LPS, desipramine, erastin, SB203580, SP600125, PDTC (Ammonium pyrrolidinedithiocarbamate), 4-PBA (Sodium phenylbutyrate), ferrostatin-1, N-acetylcysteine (NAC), and anti-α-tubulin (T9026) antibody were obtained from Sigma-Aldrich (St. Louis, MO, USA). Anti-cleaved caspase-3 (9664), anti-phospho-protein kinase R-like endoplasmic reticulum kinase (PERK) (Thr980) (3179), anti-phospho-eukaryotic translation initiation factor 2A (eIF2α) (Ser51) (3597),

anti-phospho-SAPK/JNK (Thr183/Tyr185) (9255), anti-phospho-p38 (Thr180/Tyr182) (4511), anti-phospho-p65 (Ser536) (3033), anti-soluble carrier family 7 member 11 (Slc7a11) (12691), and anti-GPX4 (59735) antibodies were purchased from Cell Signaling Technology (Beverly, MA). Anti-mouse horseradish peroxidase (HRP)-conjugated (115-036-003) and anti-rabbit HRP-conjugated (111-035-003) antibodies were procured from Jackson Laboratory (Bar Harbor, ME, USA).

PB extract

After fasting with glutinous rice flour for 2 days, PB larvae were kept in water at 25°C for 24 h for further fasting and washing. Subsequently, they were freeze-dried for 48 h and pulverized into a powder form. Then, PB extract was prepared as previously described [24]. Briefly, PB larvae powder was extracted using 70% ethanol overnight and filtered using 0.45 μm PVDF syringe filter. PB extract in 70% ethanol was diluted to a concentration of 200 mg/mL with PBS (1:5–1:20), and the protein concentration of PB extract was confirmed using the Bio-Rad Protein Assay dye reagent concentrate (Bio-Rad Laboratories, Hercules, CA, USA). PB extract was kept at −20°C for further use.

Hep3B cell, THLE-2 cell culture and treatment

Hep3B cells (hepatocellular carcinoma cell lines from 8-yrs-old black male) were grown in Dulbecco's modified Eagle medium (DMEM) (Welgene, Gyeongsan, Korea), with 10% fetal bovine serum (Welgene), 1% penicillin/streptomycin in humidified atmospheres at 37°C and subcultured every 3 days. THLE-2 cells (human normal liver cell lines) were grown in BEGM Bullet Kit (CC3170; Lonza/Clonetics Corporation, Walkersville, MD, USA). Both cells were seeded at 4×10^5 cells/well in a 6-well plate. The cells were pre-treated with 100 μg/mL of PB extract (1:2,000 dilution) for 24 h, followed by treatment with 20 μg/mL of LPS or 20 μM erastin for an additional 24 h to induce inflammation, ferroptosis and cell death. Some inhibitors (desipramine (2 μM), 4-PBA (5 mM), SB203580 (10 μM), SP600125 (10 μM), PDTC (10 μM), Ferrostatin-1 (1 μM), or NAC (10 mM)) were pre-treated before 24 h and then 20 μg/mL of LPS or 20 μM erastin was co-treated with inhibitors for another 24 h.

Western blotting

Hep3B and THLE-2 cells were lysed using RIPA buffer (50 mM Tris-HCl, pH 7.5, 150 mM NaCl, 1% Nonidet P-40, 0.5% sodium deoxycholate, and 0.1% SDS) with protease and phosphatase inhibitors (Sigma-Aldrich). The 50 μg proteins were separated on 10% SDS polyacrylamide gels and further transferred to nitrocellulose (NC) membranes (Bio-Rad Laboratories). Membranes were blocked with blocking buffer (5% bovine serum albumin (BSA) in TBST (TBS with 0.1% Tween-20) at 4°C for 1 h. Primary antibodies (1:1,000 dilutions) and secondary antibodies (1:10,000 dilutions) were sequentially attached at 4°C and at room temperature, respectively. Visualized protein bands were analyzed using the EzWestLumi Plus Reagent (ATTO Corp., Tokyo, Japan) in the ChemiDoc MP imaging system (Bio-Rad Laboratories).

MTT cell viability assay

Hep3B and THLE-2 cells were seeded at 3×10^4 cells/well in a 96-well plate. After pretreatment of PB extract or inhibitors for 24 h, cells were co-treated with 20 μg/mL of LPS or 20 μM erastin for another 20 h. The cells were incubated for additional 4 h after MTT solution (0.5 mg/mL final concentration) was added. After removing the media, purple formazan was solubilized by adding 200 μL of dimethyl sulfoxide and its concentration was determined on the optical density at 540 nm.

Enzyme-linked immunosorbent assay (ELISA)

TNF-α, interleukin (IL)-1β, and IL-6 levels were measured using TNF-α ELISA kits, IL-1β ELISA kits, and IL-6 ELISA kits (Koma Biotech, Seoul, Korea), respectively. Total ceramide levels were measured using the Human Ceramide ELISA Kit (MyBioSource, San Diego, CA, USA). Malondialdehyde (MDA) and GSH levels were analyzed using Lipid Peroxidation (MDA) Assay Kit (Abcam, Cambridge, MA, USA) and GSH Assay Kit (Biovision, Milpitas, CA, USA).

Real-time polymerase chain reaction (PCR)

Total mRNA of Hep3B cells was extracted using RNeasy Mini Kits (Qiagen, Valencia, CA, USA). cDNA was synthesized using the Verso cDNA Synthesis Kit (Thermo Scientific, Waltham, MA, USA). Quantitative PCR (qPCR) was performed on the CFX Connect Real-Time PCR Detection System (Bio-Rad Laboratories). The primers used are listed in **Table 1**.

Statistical analyses

All experiments were repeated independently in triplicate, and the data were expressed as mean ± SEM. Statistical significance was calculated using one- or two-way ANOVA and a Tukey's post hoc test (GraphPad Prism 6.0; GraphPad Software, San Diego, CA, USA).

RESULTS

PB extract prevents LPS-induced inflammation and ferroptosis in Hep3B cells

To determine proper concentration of PB extract, various concentration of PB extract was applied to Hep3B cells. Concentrations exceeding 1,500 μg/mL of PB extract induced Hep3B cell death (**Fig. 1**). Given that previous studies have utilized concentrations ranging from 10 to 300 μg/mL of PB extract [26,27], we decided to use 100 μg/mL of PB extract. Some studies have demonstrated that LPS can induce both inflammation and ferroptosis [28]. Therefore, we examined the effects of PB extracts on LPS-induced inflammation and ferroptosis. We co-treated 20 μg/mL LPS with 100 μg/mL of PB extract. PB extract reduced LPS-induced inflammatory cytokine production, such as TNF-α, IL-1β, and IL-6 (**Fig. 2A-C**), indicating that PB extract prevents LPS-induced inflammatory cytokine production. In addition, PB extract mitigated LPS-induced cell death (**Fig. 2D**) and restored GSH levels (**Fig. 2E**). PB extract also reduced LPS-induced MDA levels (**Fig. 2F**). To further understand the mechanism, we examined endoplasmic reticulum (ER) stress (phosphorylation of PERK, eif2α), MAP kinase signaling (phosphorylation of p38, JNK), NF-κB (p65 phosphorylation) and ferroptosis markers (Slc7a11, GPX4). LPS treatment increased the phosphorylation of PERK, eif2α, p38, JNK, p65 but reduced the expression of Slc7a11 and GPX4 (**Fig. 2G**). PB extract restored these levels (**Fig. 2G**), meaning that PB extract mitigated ER stress, MAP kinase signaling, inflammation and ferroptosis.

Table 1. Primers used for real-time polymerase chain reaction

Gene	Primer sequences	References
SMPD1 (ASMase)	F: 5′-TGCCAGGTTACATCGCATAG-3′	
	R: 5′-AGGTTGATGGCGGTGAATAG-3′	
SMPD2 (NSMase1)	F: 5′-CATGGTGACTGGTTCAGTGG-3′	
	R: 5′-TTGTATTCGGCATGGAGATG-3′	
SMPD3 (NSMase2)	F: 5′-GAGCAGCAACACTCCCTGTT-3′	
	R: 5′-CGTTCGTGTCCAGCAGAGTA-3′	
GAPDH	F: 5′-ACACCCACTCCTCCACCTTT-3′	[25]
	R: 5′-TGCTGTAGCCAAATTCGTTG-3′	

SMPD1, sphingomyelin phosphodiesterase 1; *ASMase*, acid sphingomyelinase; *SMPD2*, sphingomyelin phosphodiesterase 2; *NSMase1*, neutral sphingomyelinase 1; *SMPD3*, sphingomyelin phosphodiesterase 3; *NSMase2*, neutral sphingomyelinase 2; *GAPDH*, glyceraldehyde-3-phosphate dehydrogenase.
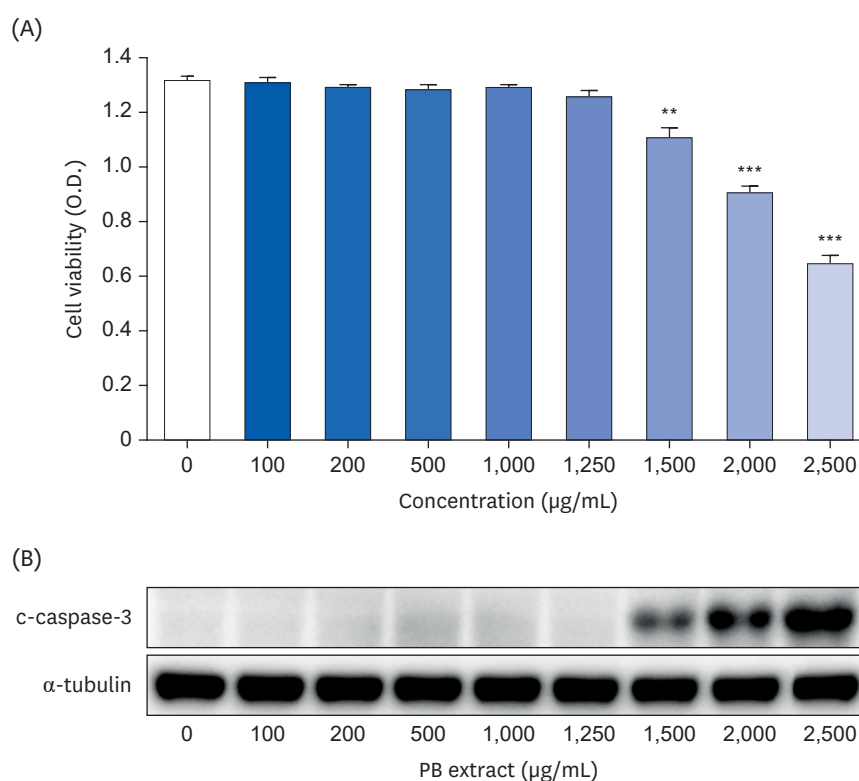
Fig. 1. Effect of PB extract on Hep3B cell death. Hep3B cells were seeded at 3×10^4 cells/well in a 96-well plate and 4×10^5 cells/well in a 6-well plate. They were treated with various concentrations of PB extract for 48 h. (A) MTT cell viability assay and (B) representative western blots of c-caspase-3 were examined. Values are expressed as mean ± SEM compared to control group. All experiments were performed in triplicate.
PB, *Protaetia brevitarsis*; c-caspase-3, cleaved caspase-3.
**$P < 0.01$, ***$P < 0.001$.

PB extract reduces LPS-induced acid SM expression in Hep3B cells

In consideration that LPS may affect ASMase [29], we examined ASMase expression in LPS-treated Hep3B cells. ASMase expression increased approximately 6-fold in LPS-treated Hep3B cells, but neither neutral sphingomyelinase (NSMase)1 nor 2 was affected (**Fig. 3A**). PB extract reduced LPS-induced ASMase expression (**Fig. 3B**), and ceramide levels (**Fig. 3C**).

To further understand whether ASMase regulates inflammation and ferroptosis, we co-treated desipramine, an ASMase inhibitor [29], with LPS. Desipramine not only reduced LPS-induced inflammatory cytokine production (TNF-α, IL-1β, and IL-6) (**Fig. 4A-C**), but also restored cell viability, GSH levels, and MDA levels (**Fig. 4D-F**). To understand the mechanism, ER stress, nuclear factor (NF)-κB, MAP kinase and ferroptosis signaling were examined. Desipramine treatment partially reduced LPS-induced phosphorylation of PERK, eif2α (ER stress), p38, JNK (MAP kinase), NF-κB p65 and it also restored the levels of Slc7a11, GPX4 (ferroptosis signaling) (**Fig. 4G**).

PB extract and desipramine reduce erastin-induced ferroptosis and cell death

Erastin can induce ferroptosis by acting as a Na⁺ independent cystine/glutamate antiporter and it also increases ASMase activity, leading to ceramide generation [17]. To further confirm whether PB extract and ASMase inhibitor (desipramine) reduce erastin-induced ferroptosis, we co-treated PB extract or desipramine with erastin. Erastin treatment reduced both Slc7a11 and GPX4 levels, but PB extract and desipramine recovered these protein levels
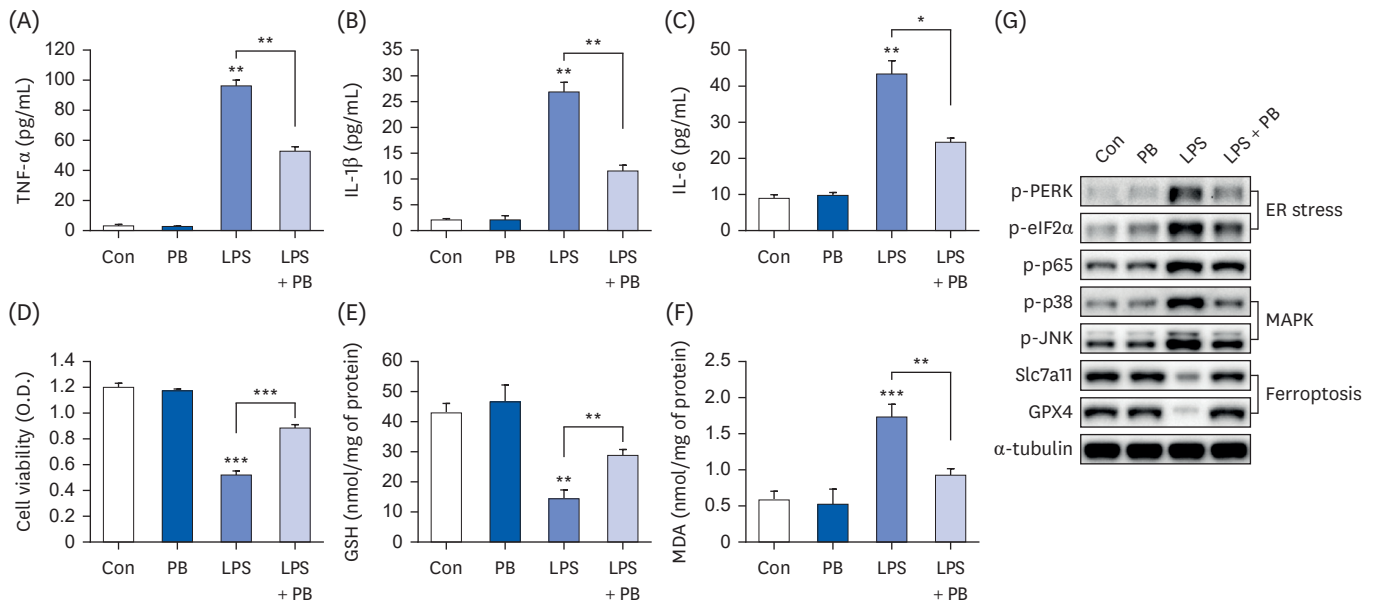
Fig. 2. PB extract reduces LPS-induced inflammation, ferroptosis and cell death. Hep3B cells were seeded at 3×10^4 cells/well in a 96-well plate and 4×10^5 cells/well in a 6-well plate. They were treated with PB extract (100 μg/mL) for 24 h, followed by 20 μg/mL LPS for another 24 h. TNF-α (A), IL-1β (B), and IL-6 (C) in cell culture media were measured using commercial enzyme-linked immunosorbent assay kits (n = 4). (D) MTT cell viability assay, (E) GSH levels, and (F) MDA levels were examined (n = 4). (G) Representative western blots of indicated proteins. Values are expressed as mean ± SEM compared to control group. All experiments were performed in triplicate.

TNF, tumor necrosis factor; Con, control (untreated); PB, *Protaetia brevitarsis*; LPS, lipopolysaccharides; IL, interleukin; GSH, glutathione; MDA, malondialdehyde; PERK, protein kinase R-like endoplasmic reticulum kinase; eIF2α, eukaryotic translation initiation factor 2A; Slc7a11, soluble carrier family 7 member 11; GPX4, glutathione peroxidase 4.
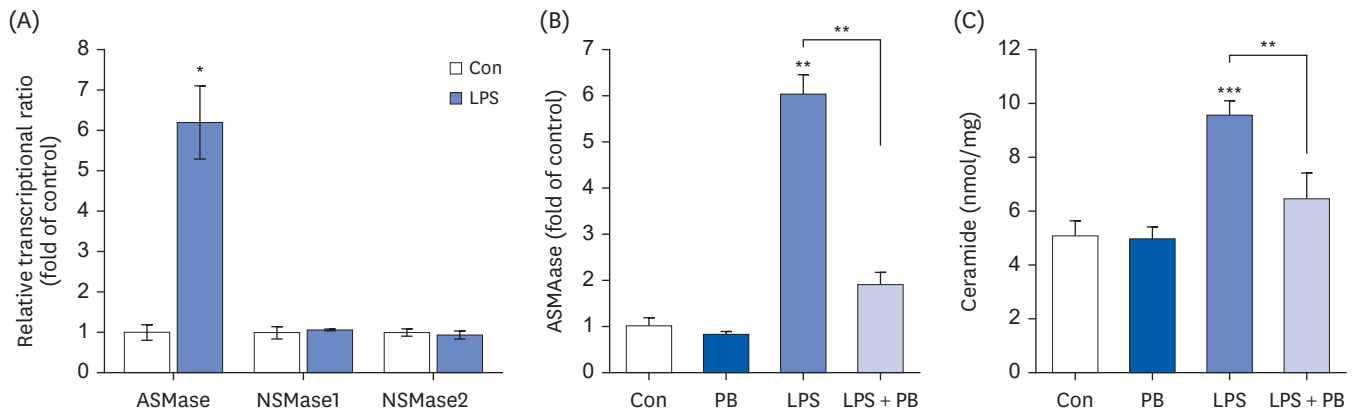$^*P < 0.05$, $^{**}P < 0.01$, $^{***}P < 0.001$.

Fig. 3. PB extract reduces LPS-induced acid sphingomyelinase expression. Hep3B cells were seeded at 3×10^4 cells/well in a 96-well plate and 4×10^5 cells/well in a 6-well plate. They were treated with PB extract (100 μg/mL) for 24 h, followed by 20 μg/mL LPS for another 24 h. (A) mRNA levels of ASMase, NSMase1, and NSMase2 after 20 μg/mL LPS treatment for 24 h in Hep3B cells. mRNA levels of ASMase (B), and ceramide levels (C) after cotreatment LPS with PB extract, (n = 4). Values are expressed as mean ± SEM compared to control group. All experiments were performed in triplicate.
Con, control (untreated); LPS, lipopolysaccharides; ASMase, acid sphingomyelinase; NSMase, neutral sphingomyelinase; PB, *Protaetia brevitarsis*.
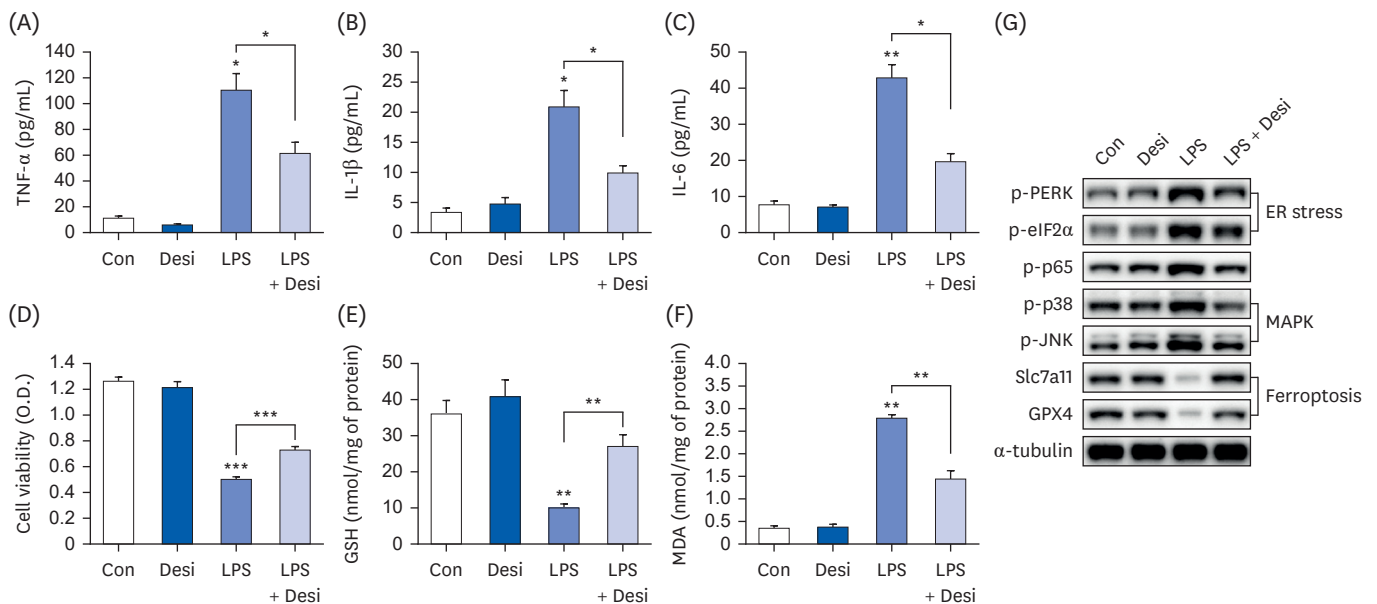$^*P < 0.05$, $^{**}P < 0.01$, $^{***}P < 0.001$.

Fig. 4. Desipramine reduces LPS-induced inflammation, ferroptosis and cell death. Hep3B cells were seeded at 3×10^4 cells/well in a 96-well plate and 4×10^5 cells/well in a 6-well plate. They were treated with desipramine (2 μM) for 24 h, followed by 20 μg/mL LPS for another 24 h. TNF-α (A), IL-1β (B), and IL-6 (C) in cell culture media were measured using commercial enzyme-linked immunosorbent assay kits (n = 4). (D) MTT cell viability assay, (E) GSH levels, and (F) MDA levels were examined (n = 4). (G) Representative western blots of indicated proteins. Values are expressed as mean ± SEM compared to control group. All experiments were performed in triplicate.
TNF, tumor necrosis factor; Con, control (untreated); Desi, desipramine; LPS, lipopolysaccharides; IL, interleukin; GSH, glutathione; MDA, malondialdehyde; PERK, protein kinase R-like endoplasmic reticulum kinase; eIF2α, eukaryotic translation initiation factor 2A; Slc7a11, soluble carrier family 7 member 11; GPX4, glutathione peroxidase 4; ER, endoplasmic reticulum.
$^*P < 0.05$, $^{**}P < 0.01$, $^{***}P < 0.001$.

(**Fig. 5A**). Similarly, erastin reduced GSH levels and increased MDA levels, but PB extract and desipramine restored these levels (**Fig. 5B and C**). PB extract and desipramine also reduced erastin-induced cell death and restored erastin-induced ceramide generation (**Fig. 5D and E**). However, erastin did not affect TNF-α production (**Fig. 5F**).

Ferroptosis/ER stress axis and inflammation are regulated by independent pathways

LPS activated multiple pathways, including ER stress (phosphorylation of PERK, eIF2α), MAP kinase signaling (JNK, p38 phosphorylation), NF-κB p65 phosphorylation, and ferroptosis. However, PB extract demonstrated a reduction in the activation of these pathways (**Fig. 2G**). To identify key pathways in LPS-induced cell death, specific inhibitors were employed. Notably, 4-PBA (an ER stress inhibitor), SB203580 (a p38 inhibitor), SP600125 (a JNK inhibitor), PDTC (a NF-κB inhibitor), and ferrostatin-1 (a ferroptosis inhibitor) were tested. SB203580, SP600125 and PDTC reduced LPS-induced cytokine production, whereas 4-PBA and ferrostatin-1 showed no effect on inflammatory cytokine production (**Fig. 6A-C**). Interestingly, 4-PBA, PDTC and ferrostatin-1 exhibited the strongest inhibition of LPS-induced cell death (**Fig. 6D**). Furthermore, only ferrostatin-1 restored GSH and MDA levels (**Fig. 6E and F**). We also analyzed ER stress (phosphorylation of PERK, eIF2α), MAP kinase signaling (phosphorylation of p38, JNK), NF-κB p65 phosphorylation, and ferroptosis after treatment of various inhibitors. Ferrostatin-1 inhibited both ER stress and ferroptosis, but 4-PBA only reduced ER stress (**Fig. 6G**), suggesting that ferroptosis acts as an upstream pathway to ER stress. SB203580, SP600125, and PDTC treatment reduced p38, JNK, and NF-κB p65 phosphorylation, respectively (**Fig. 6G**). Previous studies have shown that ROS regulate the phosphorylation of PERK [30,31]. Therefore, we treated NAC, a ROS scavenger.
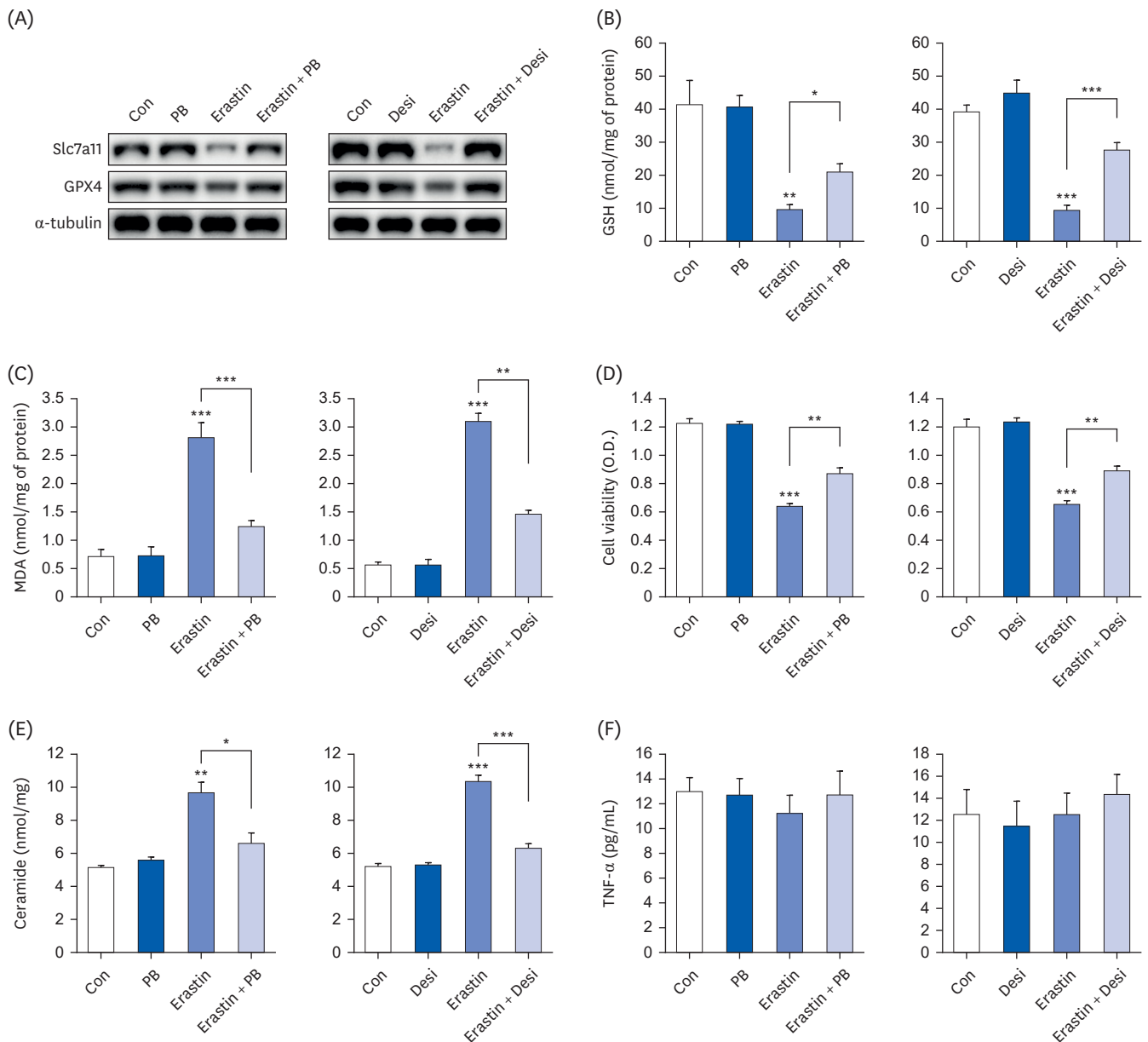
Fig. 5. PB extract and desipramine decrease erastin-induced ferroptosis and cell death. Hep3B cells were seeded at 3×10^4 cells/well in a 96-well plate and 4×10^5 cells/well in a 6-well plate. They were treated with PB extract (100 μg/mL) or desipramine (2 μM) for 24 h, followed by 20 μM erastin for another 24 h.
(A) Representative western blots of indicated proteins after erastin treatment in PB extract- or desipramine-pretreated Hep3B cells. GSH levels (B), MDA levels (C), MTT cell viability assay (D), ceramide levels (E), and TNF-α (F) were measured after erastin treatment in PB extract- or desipramine-pretreated Hep3B cells (n = 4).
Values are expressed as mean ± SEM compared to control group. All experiments were performed in triplicate.
Con, control (untreated); PB, *Protaetia brevitarsis*; Desi, desipramine; Slc7a11, soluble carrier family 7 member 11; GPX4, glutathione peroxidase 4; GSH, glutathione; MDA, malondialdehyde; TNF, tumor necrosis factor.
$^*P < 0.05$, $^{**}P < 0.01$, $^{***}P < 0.001$.

NAC treatment did not affect inflammatory cytokine production (**Fig. 7A-C**), but restored cell viability, GSH levels, and MDA levels (**Fig. 7D-F**). Similarly, NAC treatment only restored ER stress and ferroptosis, but not the phosphorylation of p38, JNK, and NF-κB p65 (**Fig. 7G**), suggesting that ROS production only affect ferroptosis and ER stress.
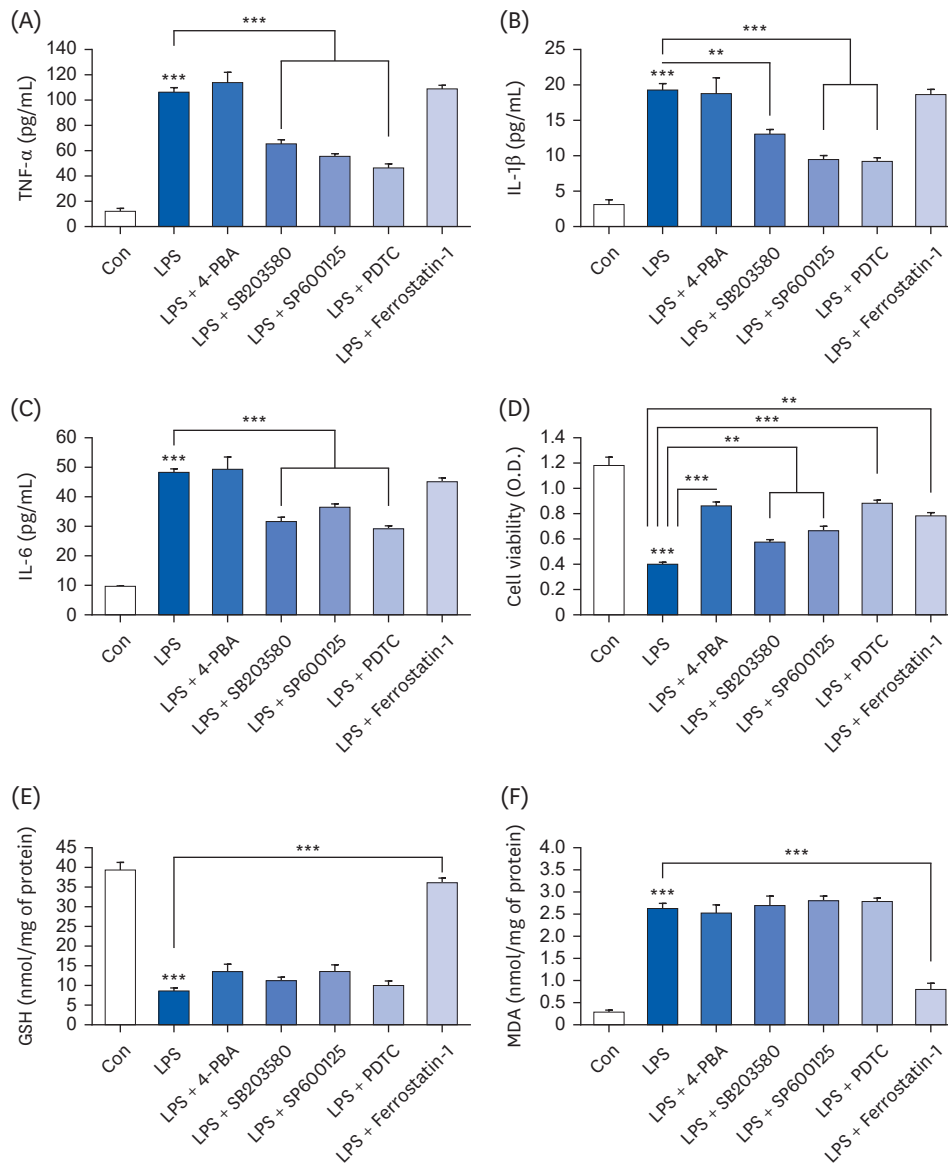

Fig. 6. Ferroptosis/ER stress and NF-κB play an important role in LPS-induced cell death. Hep3B cells were seeded at 3×10^4 cells/well in a 96-well plate and 4×10^5 cells/well in a 6-well plate. They were treated with various inhibitors (4-PBA [ER stress inhibitor, 5 mM], SB203580 [p38 inhibitor, 10 μM], SP600125 [JNK inhibitor, 10 μM], PDTC [NF-κB inhibitor, 10 μM], and ferrostatin-1 [ferroptosis inhibitor, 1 μM]) for 24 h, followed by 20 μg/mL LPS for another 24 h. TNF-α (A), IL-1β (B), and IL-6 (C) in cell culture media were measured using commercial enzyme-linked immunosorbent assay kits (n = 4). MTT cell viability assay (D), GSH levels (E), and MDA levels (F) were examined (n = 4). (G) Representative western blots of indicated proteins. Values are expressed as mean ± SEM compared to control group. All experiments were performed in triplicate.
TNF, tumor necrosis factor; Con, control (untreated); LPS, lipopolysaccharides; IL, interleukin; GSH, glutathione; MDA, malondialdehyde; ERK, protein kinase R-like endoplasmic reticulum kinase; eIF2α, eukaryotic translation initiation factor 2A; Slc7a11, soluble carrier family 7 member 11; GPX4, glutathione peroxidase 4; NF, nuclear factor.
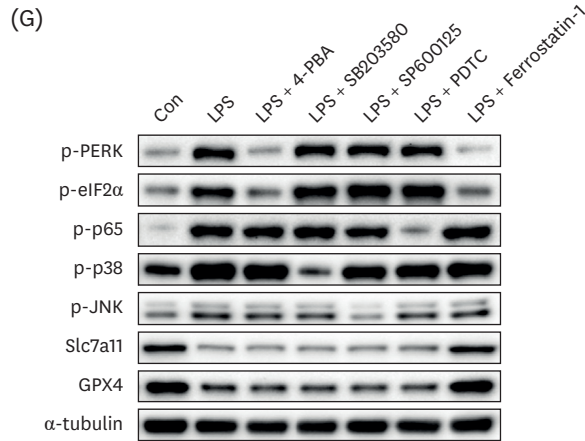**P < 0.01, ***P < 0.001.

Fig. 6. (Continued) Ferroptosis/ER stress and NF-κB play an important role in LPS-induced cell death. Hep3B cells were seeded at 3 × 10⁴ cells/well in a 96-well plate and 4 × 10⁵ cells/well in a 6-well plate. They were treated with various inhibitors (4-PBA [ER stress inhibitor, 5 mM], SB203580 [p38 inhibitor, 10 μM], SP600125 [JNK inhibitor, 10 μM], PDTC [NF-κB inhibitor, 10 μM], and ferrostatin-1 [ferroptosis inhibitor, 1 μM]) for 24 h, followed by 20 μg/mL LPS for another 24 h. TNF-α (A), IL-1β (B), and IL-6 (C) in cell culture media were measured using commercial enzyme-linked immunosorbent assay kits (n = 4). MTT cell viability assay (D), GSH levels (E), and MDA levels (F) were examined (n = 4). (G) Representative western blots of indicated proteins. Values are expressed as mean ± SEM compared to control group. All experiments were performed in triplicate.

TNF, tumor necrosis factor; Con, control (untreated); LPS, lipopolysaccharides; IL, interleukin; GSH, glutathione; MDA, malondialdehyde; ERK, protein kinase R-like endoplasmic reticulum kinase; eIF2α, eukaryotic translation initiation factor 2A; Slc7a11, soluble carrier family 7 member 11; GPX4, glutathione peroxidase 4; NF, nuclear factor.
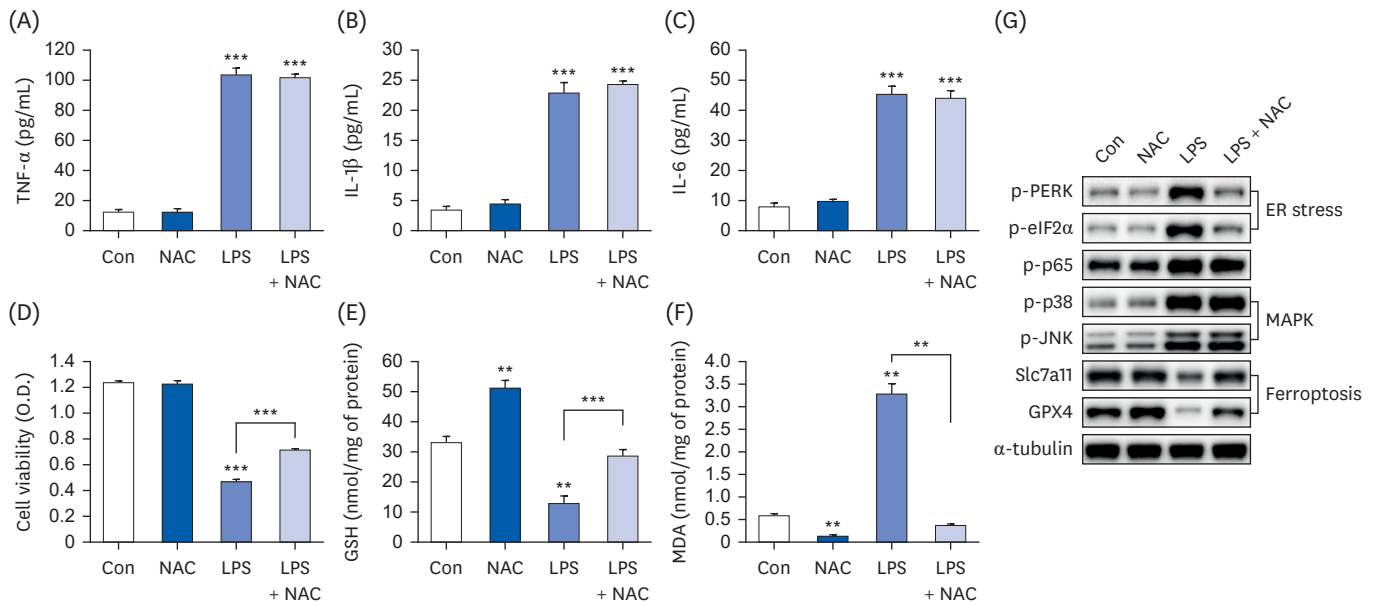$^*P < 0.05$, $^{**}P < 0.01$, $^{***}P < 0.001$.

Fig. 7. N-acetylcysteine only inhibits ferroptosis/ER stress, but not inflammatory cytokine production. Hep3B cells were seeded at 3 × 10⁴ cells/well in a 96-well plate and 4 × 10⁵ cells/well in a 6-well plate. They were treated with 10 mM NAC for 24 h, followed by 20 μg/mL LPS for another 24 h. TNF-α (A), IL-1β (B), and IL-6 (C) in cell culture media were measured using commercial enzyme-linked immunosorbent assay kits (n = 4). MTT cell viability assay (D), GSH levels (E), and MDA levels (F) were examined (n = 4). (G) Representative western blots of indicated proteins. Values are expressed as mean ± SEM compared to control group. All experiments were performed in triplicate.

TNF, tumor necrosis factor; Con, control (untreated); NAC, N-acetylcysteine; LPS, lipopolysaccharides; IL, interleukin; GSH, glutathione; MDA, malondialdehyde; PERK, protein kinase R-like endoplasmic reticulum kinase; eIF2α, eukaryotic translation initiation factor 2A; GPX4, glutathione peroxidase 4; Slc7a11, soluble carrier family 7 member 11; ER, endoplasmic reticulum.
$^{**}P < 0.01$, $^{***}P < 0.001$.

THLE-2 cell line, a type of normal liver cell, also attenuated LPS-induced ferroptosis and inflammation

Because Hep3B cells are a hepatoma cell line [32], THLE-2 cells, which are normal liver cells, were used to confirm the inhibitory effects of PB extract on LPS-induced ferroptosis and inflammation. PB extract not only reduced LPS-induced inflammatory cytokine production (TNF-α, IL-1β, and IL-6) (**Fig. 8A-C**), but also restored cell viability, GSH levels, MDA levels, ASMase expression, and ceramide levels (**Fig. 8D-H**). LPS treatment upregulated phosphorylation of PERK, eIF2α, p38, JNK, and p65 while downregulating Slc7a11 and GPX4 expression (**Fig. 8I**), which were restored by PB extract. Therefore, similar protective effects of PB extract were observed not only in Hep3B cells but also in THLE-2 cells.
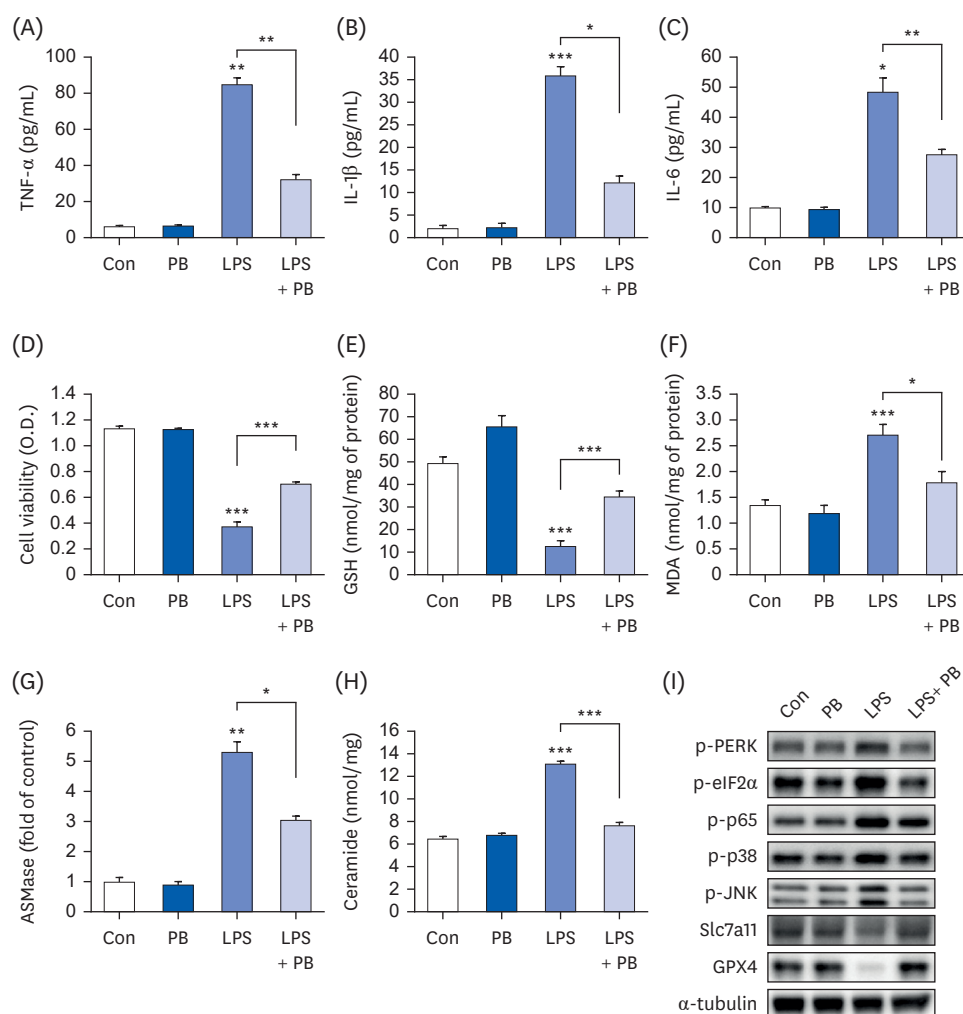

Fig. 8. PB extract reduces LPS-induced inflammation, ferroptosis and cell death in THLE-2 cells. THLE-2 cells were seeded at 3×10^4 cells/well in a 96-well plate and 4×10^5 cells/well in a 6-well plate. They were treated with PB extract (100 μg/mL) for 24 h, followed by 20 μg/mL LPS for another 24 h. TNF-α (A), IL-1β (B), and IL-6 (C) in cell culture media were measured using commercial enzyme-linked immunosorbent assay kits (n = 4). (D) MTT cell viability assay, (E) GSH levels, (F) MDA levels, (G) ASMase expression, and (H) ceramide levels were examined (n = 4). (I) Representative western blots of indicated proteins. Values are expressed as mean ± SEM compared to control group. All experiments were performed in triplicate.
TNF, tumor necrosis factor; Con, control (untreated); PB, *Protaetia brevitarsis*; LPS, lipopolysaccharides; IL, interleukin; GSH, glutathione; MDA, malondialdehyde; ASMase, acid sphingomyelinase; PERK, protein kinase R-like endoplasmic reticulum kinase; eIF2α, eukaryotic translation initiation factor 2A; Slc7a11, soluble carrier family 7 member 11; GPX4, glutathione peroxidase 4.
$^*P < 0.05$, $^{**}P < 0.01$, $^{***}P < 0.001$.

DISCUSSION

Hepatic injury is induced by many mechanisms, such as ER stress, apoptosis, inflammation, oxidative stress, and ferroptosis [28]. LPS, an inflammatory factor, was identified as a key contributor to these mechanisms, promoting ER stress, apoptosis, inflammation, and ferroptosis [28]. In our study, PB extracts demonstrated notable effects in reducing the phosphorylation of critical signaling molecules such as p65, p38 and JNK, which are implicated in the generation of inflammatory cytokines. Additionally, PB extracts exhibited a mitigating influence on ER stress and ferroptosis. PB extracts also decreased erastin-induced ferroptosis and ceramide production. These observed inhibitory effects were attributed to the downregulation of ASMase. ASMase, activated within lysosomes, rapidly releases ceramide under certain conditions, such as inflammation, ER stress, and autophagy [33]. Lysosomes can induce cell death through lysosomal membrane permeabilization (LMP), which release lysosomal contents into the cytosol, leading to cytosol acidification and damage to other organelles [34]. Ceramide, a product of ASMase activity, activates methionine adenosyltransferase (MAT1A), cathepsin D and JNK pathways, influencing processes such as autophagy, hepatic fibrosis and LMP [34]. Consequently, the downregulation of ASMase by PB extracts suggests potential anti-fibrotic and anti-inflammatory effects in hepatocytes. This implies that PB extracts may offer therapeutic benefits in mitigating hepatic injuries by modulating key pathways associated with inflammation, ferroptosis, and lysosomal function.

LPS triggers diverse signaling pathways, including ER stress, MAP kinase, NF-κB and ferroptosis. Among the inhibitors tested, those targeting ER stress, NF-κB p65, and ferroptosis demonstrated the most significant reduction in cell death. Ferroptosis inhibitor, ferrostatin-1, inhibited not only ferroptosis, but also ER stress. However, ER stress inhibitor, 4-PBA, only mitigated ER stress without impacting ferroptosis, suggesting that ferroptosis acts upstream of ER stress. Previous studies have shown that ROS induced PERK phosphorylation [30,31], indicating that ROS generated by LPS affect both ER stress and ferroptosis. However, inflammation is primarily induced by MAP kinase (p38, JNK) and NF-κB p65. Treatment with SB203580, SP600125, and PDTC effectively reduced LPS-induced inflammatory cytokine production, but these inhibitors did not affect ER stress and ferroptosis. These findings collectively suggest that ferroptosis/ER stress and inflammation do not reciprocally influence each other (**Fig. 9**). Thus, ASMase activates ferroptosis, which subsequently triggers ER stress. Additionally, LPS-induced inflammation is activated by NF-κB p65, MAP kinase (p38, JNK).

There have been no studies on ferroptosis in edible insects, and this study represents the first investigation into ferroptosis. However, numerous edible insects have anti-inflammatory and anti-ferroptosis properties; for example, *T. molitor* larvae and *Gryllus bimaculatus* have demonstrated anti-inflammatory properties in several studies [35,36]. Additionally, PB also has been identified as having anti-inflammatory effects, and reduced p65 phosphorylation [37]. In another study, PB paste and sauce extracts restored ethanol-induced GSH levels and superoxide dismutase protein levels, meaning that these exhibit antioxidant effects [21]. Similarly, other edible insects, such as *T. molitor* larvae and *G. bimaculatus*, have been found to possess antioxidant effects [22,23]. Therefore, most edible insects likely exhibit anti-ferroptosis effects owing to their antioxidant properties. However, in this study, only Hep3B cells and THLE-2 cells were used to study the anti-inflammatory and anti-ferroptosis properties of PB extracts. Therefore, these effects need to be further validated in animal and human studies, as well as in other cell lines. The PB extracts, which were prepared using 70%
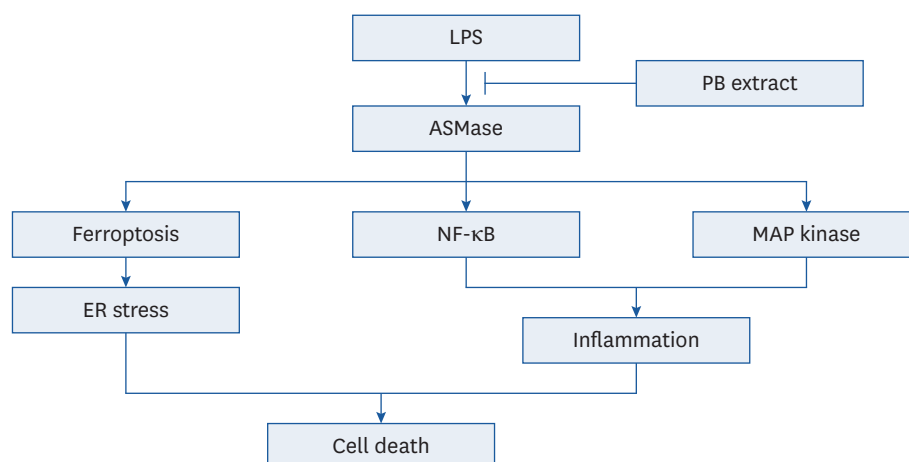
Fig. 9. Schematic showing the effects of PB extract in LPS-induced cell death. LPS induced ASMase activation, initiating a cascade that triggers ferroptosis, NF-κB, and MAP kinase pathways. Ferroptosis promotes ER stress, while NF-κB and MAP kinase pathways contribute to increased inflammation. Both pathways finally lead to cell death. PB extract inhibits ASMase activation, effectively inhibiting all these pathways and preventing cell death. LPS, lipopolysaccharides; PB, *Protaetia brevitarsis*; ASMase, acid sphingomyelinase; NF, nuclear factor; ER, endoplasmic reticulum.

ethanol, are expected to contain various compounds, such as proteins, fatty acids, and other substances. Further experiments will be needed to isolate beneficial compounds with anti-inflammatory and anti-ferroptosis functions from these substances.

PB extract shows promising therapeutic potential in mitigating hepatic injuries by targeting key pathways associated with inflammation, ferroptosis, and ER stress. The observed downregulation of ASMase not only reduces ferroptosis and ER stress, but also reduces inflammatory cytokine production via MAP kinase, NF-kB p65. This study not only unveils a novel investigation into ferroptosis in edible insects but also underscores the potential anti-inflammatory and antioxidant effects of PB, suggesting its application in hepatic health interventions.

REFERENCES

1. Jantzen da Silva Lucas A, Menegon de Oliveira L, da Rocha M, Prentice C. Edible insects: An alternative of nutritional, functional and bioactive compounds. Food Chem 2020;311:126022. **PUBMED** | **CROSSREF**

2. Boehm E, Borzekowski D, Ververis E, Lohmann M, Böl GF. Communicating food risk-benefit assessments: edible insects as red meat replacers. Front Nutr 2021;8:749696. **PUBMED** | **CROSSREF**

3. Saeb A, Grundmann SM, Gessner DK, Schuchardt S, Most E, Wen G, Eder K, Ringseis R. Feeding of cuticles from *Tenebrio molitor* larvae modulates the gut microbiota and attenuates hepatic steatosis in obese Zucker rats. Food Funct 2022;13:1421-36. **PUBMED** | **CROSSREF**

4. Seo M, Goo TW, Chung MY, Baek M, Hwang JS, Kim MA, Yun EY. *Tenebrio molitor* larvae inhibit adipogenesis through AMPK and MAPKs signaling in 3T3-L1 adipocytes and obesity in high-fat diet-induced obese mice. Int J Mol Sci 2017;18:518. **PUBMED** | **CROSSREF**

5. Yu JM, Jang JY, Kim HJ, Cho YH, Kim D, Kwon O, Cho YJ, An BJ. Antioxidant capacity and Raw 264.7 macrophage anti-inflammatory effect of the *Tenebrio molitor*. Korean Journal of Food Preservation 2016;23:890-8. **CROSSREF**

6. Ahn EM, Myung NY, Jung HA, Kim SJ. The ameliorative effect of *Protaetia brevitarsis* larvae in HFD-induced obese mice. Food Sci Biotechnol 2019;28:1177-86. **PUBMED** | **CROSSREF**

7. Park CE, Lee SO. Nrf2-mediated protective effect of protein hydrolysates from *Protaetia brevitarsis* larvae against oxidative stress-induced hepatotoxicity. Food Sci Biotechnol 2023;32:1561-71. **PUBMED** | **CROSSREF**

8. Jang HY, Kim JM, Kim JS, Kim BS, Lee YR, Bae JS. *Protaetia brevitarsis* extract attenuates RANKL-induced osteoclastogenesis by inhibiting the JNK/NF-κB/PLCγ2 signaling pathway. Nutrients 2023;15:3193. **CROSSREF**

9. MacKichan ML, DeFranco AL. Role of ceramide in lipopolysaccharide (LPS)-induced signaling. LPS increases ceramide rather than acting as a structural homolog. J Biol Chem 1999;274:1767-75. **PUBMED** | **CROSSREF**

10. Xiang H, Jin S, Tan F, Xu Y, Lu Y, Wu T. Physiological functions and therapeutic applications of neutral sphingomyelinase and acid sphingomyelinase. Biomed Pharmacother 2021;139:111610. **PUBMED** | **CROSSREF**

11. García-Ruiz C, Colell A, Marí M, Morales A, Calvo M, Enrich C, Fernández-Checa JC. Defective TNF-alpha-mediated hepatocellular apoptosis and liver damage in acidic sphingomyelinase knockout mice. J Clin Invest 2003;111:197-208. **PUBMED** | **CROSSREF**

12. Fernandez A, Matias N, Fucho R, Ribas V, Von Montfort C, Nuño N, Baulies A, Martinez L, Tarrats N, Mari M, et al. ASMase is required for chronic alcohol induced hepatic endoplasmic reticulum stress and mitochondrial cholesterol loading. J Hepatol 2013;59:805-13. **PUBMED** | **CROSSREF**

13. Lang PA, Schenck M, Nicolay JP, Becker JU, Kempe DS, Lupescu A, Koka S, Eisele K, Klarl BA, Rübben H, et al. Liver cell death and anemia in Wilson disease involve acid sphingomyelinase and ceramide. Nat Med 2007;13:164-70. **PUBMED** | **CROSSREF**

14. Osawa Y, Seki E, Adachi M, Suetsugu A, Ito H, Moriwaki H, Seishima M, Nagaki M. Role of acid sphingomyelinase of Kupffer cells in cholestatic liver injury in mice. Hepatology 2010;51:237-45. **PUBMED** | **CROSSREF**

15. Moles A, Tarrats N, Morales A, Domínguez M, Bataller R, Caballería J, García-Ruiz C, Fernández-Checa JC, Marí M. Acidic sphingomyelinase controls hepatic stellate cell activation and *in vivo* liver fibrogenesis. Am J Pathol 2010;177:1214-24. **PUBMED** | **CROSSREF**

16. Mir IH, Thirunavukkarasu C. The relevance of acid sphingomyelinase as a potential target for therapeutic intervention in hepatic disorders: current scenario and anticipated trends. Arch Toxicol 2023;97:2069-87. **PUBMED** | **CROSSREF**

17. Thayyullathil F, Cheratta AR, Alakkal A, Subburayan K, Pallichankandy S, Hannun YA, Galadari S. Acid sphingomyelinase-dependent autophagic degradation of GPX4 is critical for the execution of ferroptosis. Cell Death Dis 2021;12:26. **PUBMED** | **CROSSREF**

18. Du YX, Zhao YT, Sun YX, Xu AH. Acid sphingomyelinase mediates ferroptosis induced by high glucose via autophagic degradation of GPX4 in type 2 diabetic osteoporosis. Mol Med 2023;29:125. **PUBMED** | **CROSSREF**

19. Xie Y, Hou W, Song X, Yu Y, Huang J, Sun X, Kang R, Tang D. Ferroptosis: process and function. Cell Death Differ 2016;23:369-79. **PUBMED** | **CROSSREF**

20. Yang WS, Kim KJ, Gaschler MM, Patel M, Shchepinov MS, Stockwell BR. Peroxidation of polyunsaturated fatty acids by lipoxygenases drives ferroptosis. Proc Natl Acad Sci U S A 2016;113:E4966-75. **PUBMED** | **CROSSREF**

21. Hwang D, Goo TW, Yun EY. In Vitro Protective Effect of Paste and Sauce Extract Made with Protaetia brevitarsis Larvae on HepG2 Cells Damaged by Ethanol. Insects 2020;11.

22. Ganguly K, Dutta SD, Jeong MS, Patel DK, Cho SJ, Lim KT. Naturally-derived protein extract from *Gryllus bimaculatus* improves antioxidant properties and promotes osteogenic differentiation of hBMSCs. PLoS One 2021;16:e0249291. **PUBMED** | **CROSSREF**

23. Navarro del Hierro J, Gutiérrez-Docio A, Otero P, Reglero G, Martin D. Characterization, antioxidant activity, and inhibitory effect on pancreatic lipase of extracts from the edible insects *Acheta domesticus* and *Tenebrio molitor*. Food Chem 2020;309:125742. **PUBMED** | **CROSSREF**

24. Kim MH, Kim SJ, Kim SH, Park WJ, Han JS. *Gryllus bimaculatus*-containing diets protect against dexamethasone-induced muscle atrophy, but not high-fat diet-induced obesity. Food Sci Nutr 2023;11:2787-97. **PUBMED** | **CROSSREF**

25. Kim MH, Park JW, Lee EJ, Kim S, Shin SH, Ahn JH, Jung Y, Park I, Park WJ. C16-ceramide and sphingosine 1-phosphate/S1PR2 have opposite effects on cell growth through mTOR signaling pathway regulation. Oncol Rep 2018;40:2977-87. **PUBMED** | **CROSSREF**

26. Choi RY, Kim IW, Ji M, Paik MJ, Ban EJ, Lee JH, Hwang JS, Kweon H, Seo M. *Protaetia brevitarsis seulensis* larvae ethanol extract inhibits RANKL-stimulated osteoclastogenesis and ameliorates bone loss in ovariectomized mice. Biomed Pharmacother 2023;165:115112. **PUBMED** | **CROSSREF**

27. Park YM, Noh EM, Lee HY, Shin DY, Lee YH, Kang YG, Na EJ, Kim JH, Yang HJ, Kim MJ, et al. Anti-diabetic effects of Protaetia brevitarsis in pancreatic islets and a murine diabetic model. Eur Rev Med Pharmacol Sci 2021;25:7508-15. **PUBMED**

28. Zhao C, Xiao C, Feng S, Bai J. Artemisitene alters LPS-induced oxidative stress, inflammation and ferroptosis in liver through Nrf2/HO-1 and NF-kB pathway. Front Pharmacol 2023;14:1177542. **PUBMED** | **CROSSREF**

29. Kim MH, Ahn HK, Lee EJ, Kim SJ, Kim YR, Park JW, Park WJ. Hepatic inflammatory cytokine production can be regulated by modulating sphingomyelinase and ceramide synthase 6. Int J Mol Med 2017;39:453-62. **PUBMED** | **CROSSREF**

30. Yin L, Dai Y, Cui Z, Jiang X, Liu W, Han F, Lin A, Cao J, Liu J. The regulation of cellular apoptosis by the ROS-triggered PERK/EIF2α/chop pathway plays a vital role in bisphenol A-induced male reproductive toxicity. Toxicol Appl Pharmacol 2017;314:98-108. **PUBMED** | **CROSSREF**

31. Sun J, Chen W, Li S, Yang S, Zhang Y, Hu X, Qiu H, Wu J, Xu S, Chu T. Nox4 promotes RANKL-induced autophagy and osteoclastogenesis via activating ROS/PERK/eIF-2α/ATF4 pathway. Front Pharmacol 2021;12:751845. **PUBMED** | **CROSSREF**

32. Rodríguez-Hernández MA, Chapresto-Garzón R, Cadenas M, Navarro-Villarán E, Negrete M, Gómez-Bravo MA, Victor VM, Padillo FJ, Muntané J. Differential effectiveness of tyrosine kinase inhibitors in 2D/3D culture according to cell differentiation, p53 status and mitochondrial respiration in liver cancer cells. Cell Death Dis 2020;11:339. **PUBMED** | **CROSSREF**

33. Jenkins RW, Canals D, Hannun YA. Roles and regulation of secretory and lysosomal acid sphingomyelinase. Cell Signal 2009;21:836-46. **PUBMED** | **CROSSREF**

34. Insausti-Urkia N, Solsona-Vilarrasa E, Garcia-Ruiz C, Fernandez-Checa JC. Sphingomyelinases and liver diseases. Biomolecules 2020;10:1497. **PUBMED** | **CROSSREF**

35. Oh E, Park WJ, Kim Y. Effects of *Tenebrio molitor* larvae and its protein derivatives on the antioxidant and anti-inflammatory capacities of tofu. Food Biosci 2022;50:102105. **CROSSREF**

36. Park WJ, Han JS. *Gryllus bimaculatus* extract protects against lipopolysaccharide and palmitate-induced production of proinflammatory cytokines and inflammasome formation. Mol Med Rep 2021;23:206. **PUBMED** | **CROSSREF**

37. Choi YJ, Bae IY. White-spotted flower chafer (*Protaetia brevitarsis*) ameliorates inflammatory responses in LPS-stimulated RAW 264.7 macrophages. J Insects Food Feed 2023;9:1037-46. **CROSSREF**